pharmaceuticals

Article

Chronic Propafenone Application Increases Functional $K_{IR}2.1$ Expression In Vitro

Encan Li, Willy Kool, Liset Woolschot and Marcel A. G. van der Heyden *

Department of Medical Physiology, Division of Heart & Lungs, University Medical Center Utrecht, Yalelaan 50, 3584 CM Utrecht, The Netherlands

* Correspondence: m.a.g.vanderheyden@umcutrecht.nl; Tel.: +31-88-755-8900

Abstract: Expression and activity of inwardly rectifying potassium (K_{IR}) channels within the heart are strictly regulated. K_{IR} channels have an important role in shaping cardiac action potentials, having a limited conductance at depolarized potentials but contributing to the final stage of repolarization and resting membrane stability. Impaired $K_{IR}2.1$ function causes Andersen-Tawil Syndrome (ATS) and is associated with heart failure. Restoring $K_{IR}2.1$ function by agonists of $K_{IR}2.1$ (AgoKirs) would be beneficial. The class 1c antiarrhythmic drug propafenone is identified as an AgoKir; however, its long-term effects on $K_{IR}2.1$ protein expression, subcellular localization, and function are unknown. Propafenone's long-term effect on $K_{IR}2.1$ expression and its underlying mechanisms in vitro were investigated. $K_{IR}2.1$-carried currents were measured by single-cell patch-clamp electrophysiology. $K_{IR}2.1$ protein expression levels were determined by Western blot analysis, whereas conventional immunofluorescence and advanced live-imaging microscopy were used to assess the subcellular localization of $K_{IR}2.1$ proteins. Acute propafenone treatment at low concentrations supports the ability of propafenone to function as an AgoKir without disturbing $K_{IR}2.1$ protein handling. Chronic propafenone treatment (at 25–100 times higher concentrations than in the acute treatment) increases $K_{IR}2.1$ protein expression and $K_{IR}2.1$ current densities in vitro, which are potentially associated with pre-lysosomal trafficking inhibition.

Keywords: $K_{IR}2.1$; AgoKir; long-term effects; propafenone; trafficking

Citation: Li, E.; Kool, W.; Woolschot, L.; van der Heyden, M.A.G. Chronic Propafenone Application Increases Functional $K_{IR}2.1$ Expression In Vitro. *Pharmaceuticals* **2023**, *16*, 404. https://doi.org/10.3390/ph16030404

Academic Editor: Giorgio Cozza

Received: 10 February 2023
Revised: 28 February 2023
Accepted: 4 March 2023
Published: 7 March 2023

1. Introduction

Inward rectification was first detected in 1949 by Bernard Katz [1]. At first, it was called "anomalous rectification" to distinguish it from voltage-gated K (Kv) channel current in squid giant axons [2,3]. Since then, significant progress has been made in this area of research. These developments include cloning the members of inward rectifier channels, discovering the molecular mechanism of inward rectification, implementing genetic studies in experimental animals, constructing mutations in inward rectifier genes, and so on [4–10]. The $K_{IR}2.1$ channel protein is encoded by *KCNJ2*, and $K_{IR}2.1$ current is a major part of the inward rectifying potassium current (IK_1) in cardiomyocytes, as no detectable current was observed in ventricular myocytes from $K_{IR}2.1$ knockout mice [2,11,12]. IK_1 generated by $K_{IR}2.x$ channels ($K_{IR}2.1$, $K_{IR}2.2$, and $K_{IR}2.3$ homo- and heterotetramers) is responsible for controlling the resting membrane potential and accelerating the final repolarization phase in cardiomyocytes [2,13]. Therefore, regulating the IK_1 current can greatly affect the excitability and arrhythmogenesis of cardiomyocytes [13,14]. Recent findings and the development of new compounds may yield new pharmacological IK_1 modulators [10,15–17].

The strong inward rectification of $K_{IR}2.1$ channels mainly results from the interaction with intracellular polyamines as they block the outflux of K^+ by binding to the negatively charged residues in the transmembrane (D172) and cytoplasmic domain (E224, E229) of the channel [2,4,6,7,13,18–22]. Gain-of-function in $K_{IR}2.1$ can cause atrial fibrillation [14,23]. On the contrary, dysfunction of $K_{IR}2.1$ can prolong the duration of the cardiac action potential,

which can cause Andersen-Tawil Syndrome (ATS) [14,24–27]. Furthermore, heart failure is associated with decreased IK_1 density [28]. For the latter situations, restoration of normal $K_{IR}2.1$ function by agonists of $K_{IR}2.1$ (AgoKirs) would be beneficial [29].

The drug propafenone—an orally active sodium channel blocking agent—was identified as an AgoKir [29,30]. It is currently used as a class Ic antiarrhythmic drug [31,32]. Previous experiments revealed that low concentrations (0.5–1 μM) of propafenone acutely increase IK_1 by binding with Cys311 of the $K_{IR}2.1$ protein [29–31,33]. Since the effect of propafenone on IK_1 generated by $K_{IR}2.1$ is acute, it implies that chronic treatment will be needed in patients to obtain a permanent benefit. It has been established that drugs influencing ion channel activity directly could also alter ion channel expression and function in the long-term [34,35]. However, the long-term influence of propafenone on $K_{IR}2.1$ channels is unknown. Therefore, we explored whether propafenone affects $K_{IR}2.1$ expression, its subcellular localization, and its functional consequence in the long-term.

In the current work, we confirm that propafenone can act as an AgoKir. We explored the long-term effects of propafenone on IK_1 and $K_{IR}2.1$, but also its close homologue $K_{IR}2.2$, channel expressions. Live imaging was also performed to determine the subcellular localization of $K_{IR}2.1$ proteins. As $K_{IR}2.1$ channel proteins degrade via the lysosomal pathway [36], the half-life of the protein in the presence of propafenone was determined [36–38]. This study provides a basis for further research on propafenone-based AgoKirs, thus contributing to the development of a therapy for diseases in which the function of $K_{IR}2.1$ is reduced.

2. Results

2.1. As an AgoKir, Propafenone Can Increase Both Channel Expression and IK_1 Density

To confirm that propafenone could increase $K_{IR}2.1$ channel generated IK_1, the acute effects of low doses of propafenone on IK_1 were investigated by whole-cell patch-clamping in HEK-KWGF cells. Analyses were performed separately for each measured voltage point. Statistical analysis showed that the outward component of (−60 to −20 mV) IK_1 was increased, especially at −40 mV, when compared with the control upon perfusion with 1 μM propafenone (Figure S1). Whereas, at a concentration of 25 μM, both the inward and outward components are decreased (Figure S1). Similar results had been found previously [30].

Next, the long-term effects of propafenone on IK_1 and $K_{IR}2.1$ and $K_{IR}2.2$ protein expression were explored. Figure 1A,B show that propafenone can increase the expression levels of $K_{IR}2.1$ and $K_{IR}2.2$ proteins dose-dependently. To see whether the increased protein levels observed by western blot would also result in increased expression levels on the membrane and $K_{IR}2.1$-carried current, we treated HEK-KWGF cells with 50 μM propafenone for 24 h and analyzed them immediately for IK_1 current densities in the absence of propafenone (Figure 1C). Long-term treatment of the cells with propafenone significantly increased both the inward component of IK_1 at membrane potentials between −120 and −100 mV and the outward component at membrane potentials between −70 and 30 mV.

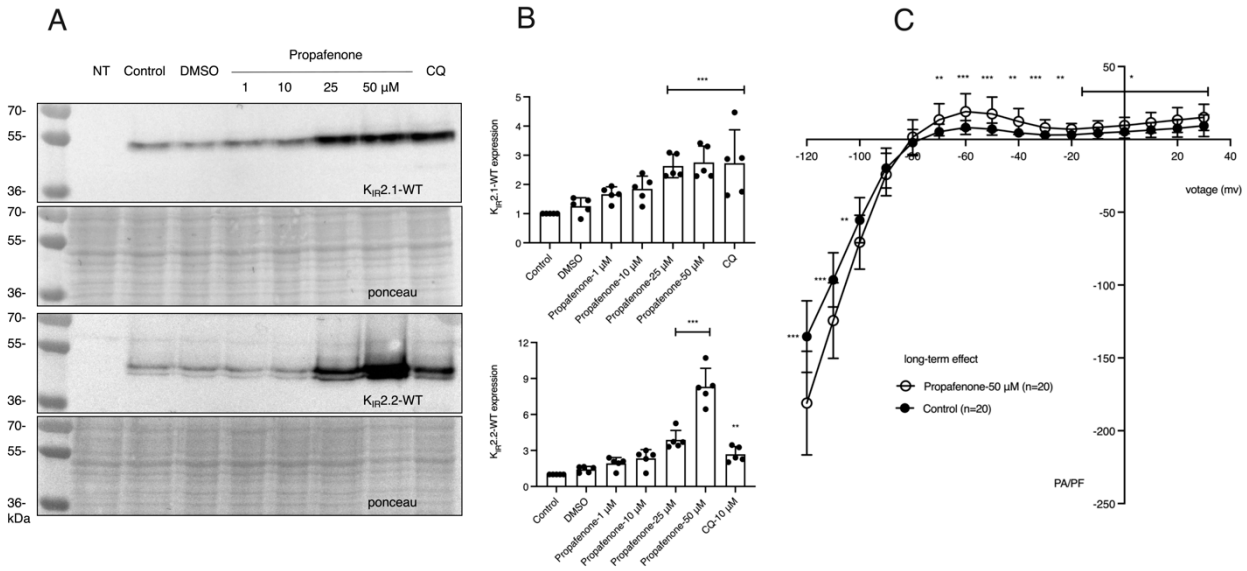

Figure 1. 24 h effects of propafenone on K_{IR}2.x expression and function. (**A**) Western blot analysis of human WT K_{IR}2.1 and K_{IR}2.2 expression in HEK-293 cells. Cells were treated with different concentrations of propafenone (1, 10, 25, 50 μM) for 24 h (n = 5). Non-transfected cells (NT) were used as a negative control. (**B**) Summarized results of K_{IR}2.1 and K_{IR}2.2 expression in control and cells treated for propafenone (n = 5). The control protein level was set at 1 after correction for loading. Ponceau staining was used as a loading control. (**C**) Propafenone treatment increased both inward and outward $I_{KIR2.1}$ in HEK-KWGF cells. Current-voltage relationship of mean $I_{KIR2.1}$ current values ± SD, measured in the absence of propafenone. In the treatment group, cells were pretreated with propafenone for 24 h with a final concentration of 50 μM. The control group did not undergo any treatment. n = 20 cells for each group. Lysosomal inhibitor chloroquine, CQ, is used as a positive control. * $p < 0.05$, ** $p < 0.01$, *** $p < 0.001$ vs. control.

2.2. Propafenone Specifically Works on K_{IR}2.1 Channels and Shows a Long Residence Time

After determining the long-term effect of propafenone on K_{IR}2.1 channel expression, we next investigated hERG (K_v11.1) and sodium channels (Na_v1.5) to test if propafenone has a similar effect on other channel protein types over the same time period. HEK-hERG cells and HEK-Na_v1.5 cells were used. As the HEK-Na_v1.5 cell line stably expresses both Na_v1.5 and K_{IR}2.1 channels, we determined Na_v1.5 protein expression alongside K_{IR}2.1 expression levels from the same samples. As shown in Figure 2A,B, the expression levels of Na_v1.5 and K_v11.1 channel proteins did not change in response to propafenone treatment. The expression level of K_{IR}2.1 protein was increased similarly, as shown in Figure 1A, which indicates that propafenone can specifically work on K_{IR} channels, even in the presence of another ectopically expressed ion channel (i.e., Na_v1.5).

To determine the retention time of propafenone's effect on K_{IR}2.1 expression levels following drug removal, a washout experiment was performed. The expression levels of K_{IR}2.1 proteins decreased significantly after washout, showing propafenone's washout effect (Figure 3A,B). However, for the cells that received treatment with 50 μM propafenone, the expression of K_{IR}2.1 remained high after washout for 24 h (Figure 3A,B). This long residence time (24 h) indicates the persistence of propafenone's chronic effect.

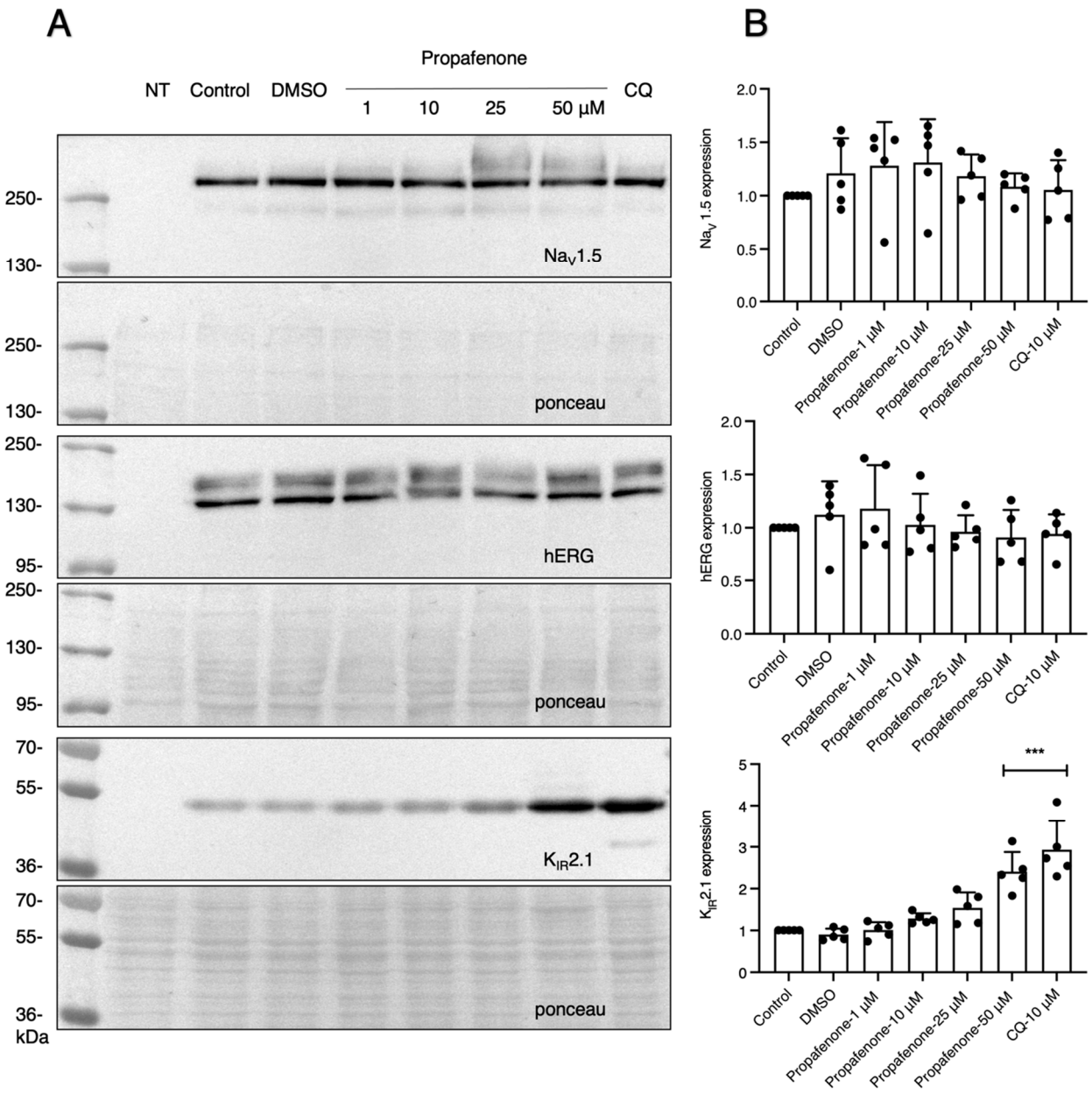

Figure 2. Propafenone specificity for K_{IR} channels. (**A**) Western blot analysis of hERG channel protein, sodium channel protein, and $K_{IR}2.1$ channel protein expression levels. $K_v11.1$ is a voltage-activated potassium channel expressed as a core N-glycosylated immature form (~135 kDa) and a fully N-glycosylated mature form (~155 kDa) in HEK-hERG cells [39]. $Na_v1.5$ is a voltage-activated sodium channel expressed as a single band (~250 kDa) in the HEK-$Na_v1.5$ cells [40]. Cells were treated with different concentrations of propafenone (1, 10, 25, and 50 μM) for 24 h (n = 5). Non-transfected cells (NT) were used as a negative control. (**B**) Summarized results of (**A**) (n = 5). The control protein level was set at 1 after correction for loading. Ponceau staining was used as a loading control. *** $p < 0.001$ vs. control.

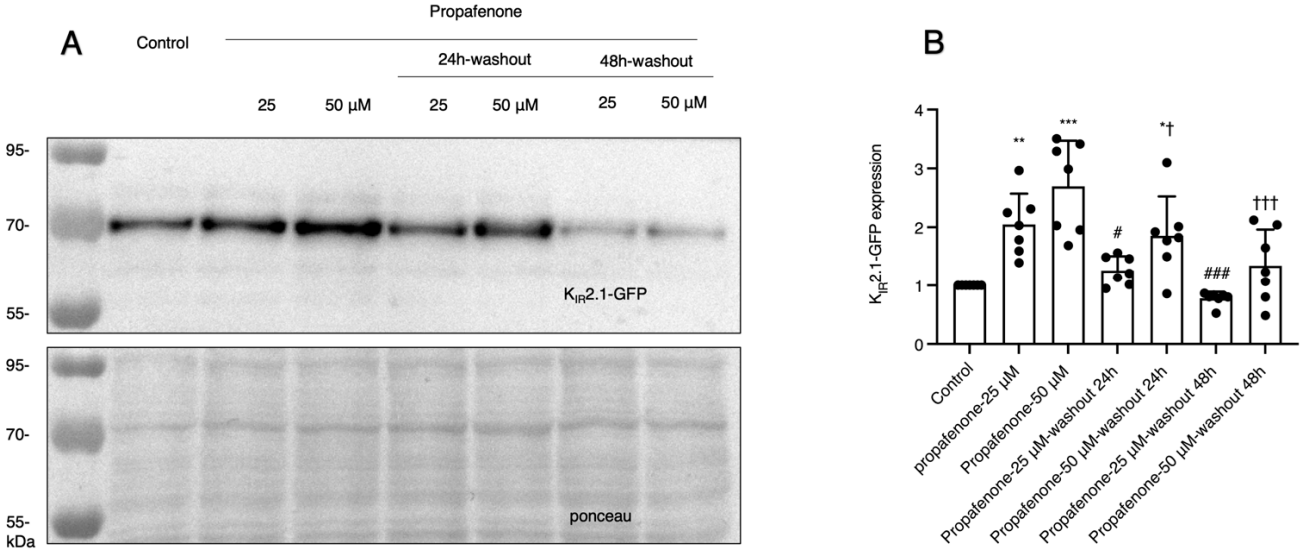

Figure 3. Washout effect of propafenone on $K_{IR}2.1$ expression. (**A**) $K_{IR}2.1$ expression before and after washout (n = 7). (**B**) Summarized results of (**A**). The control protein level was set at 1 after correction for loading. Ponceau staining was used as a loading control. * $p < 0.05$, ** $p < 0.01$, *** $p < 0.001$ vs. control; # $p < 0.05$, ### $p < 0.001$ vs. propafenone-25 μM group; † $p < 0.05$, ††† $p < 0.001$ vs. propafenone 50 μM group.

2.3. Channel Function, Polyamine Binding Sites, and the Drug-Channel Interaction Location Do Not Interfere with the Long-Term Effect of Propafenone on $K_{IR}2.1$ Expression

As IK_1 current plays an important role in regulating various physiological processes, it is essential to know whether channel functions were involved in the long-term effect of propafenone. We used a $K_{IR}2.1$-AAA non-conducting channel protein. In addition, $BaCl_2$ was used as a channel-blocking agent. It demonstrated that the expression of $K_{IR}2.1$ proteins was increased similarly as compared to WT at higher concentrations of propafenone (50 μM), while IK_1 was inactivated by the $K_{IR}2.1$-AAA mutation or blocked by $BaCl_2$ (Figure 4A,B). Since polyamine binding sites (D172, E299, and E244) play important roles in the inward rectification of $K_{IR}2.1$ channels and direct drug-channel interference is indispensable in the acute reactions of propafenone [2,29], we further investigated the roles of these factors. Western blots showed similar effects for these mutant proteins when compared with WT (Figure 5).

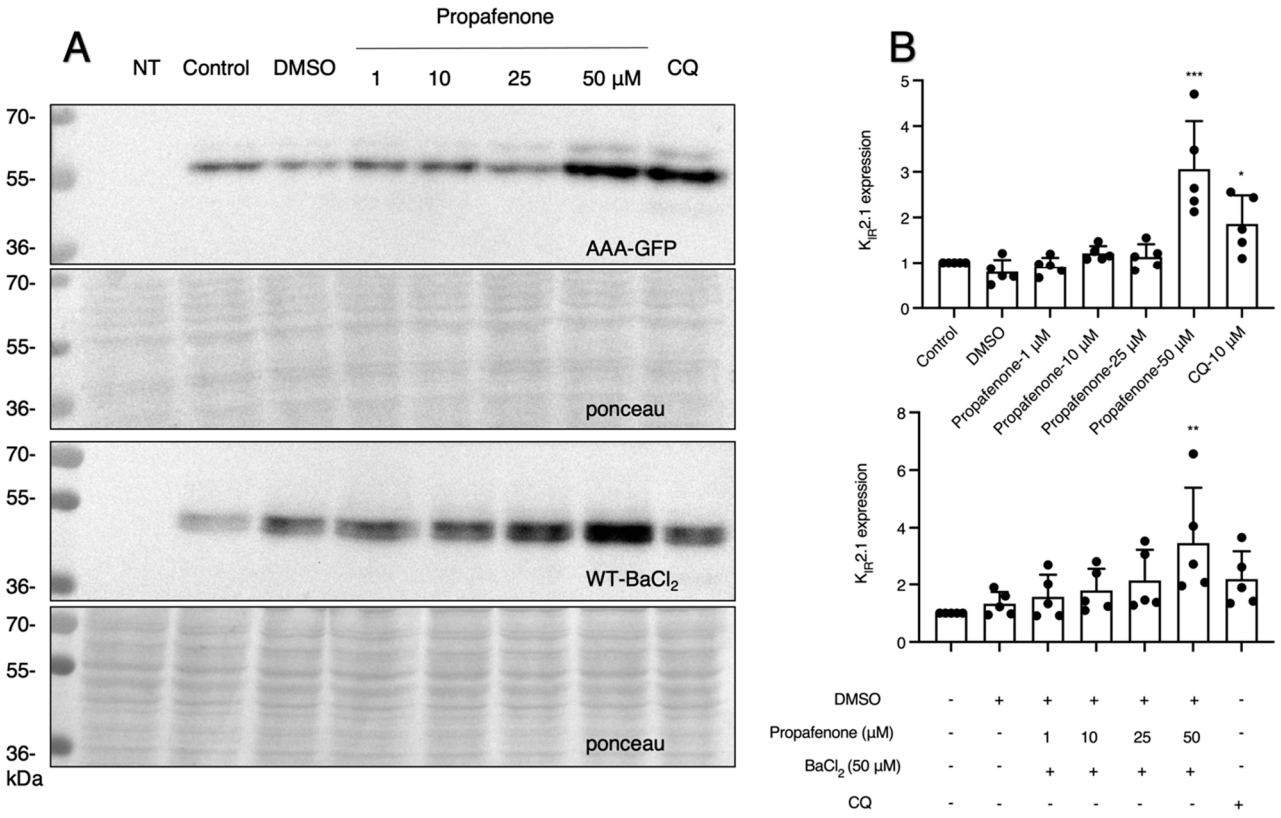

Figure 4. Channel function does not affect the changes in expression of $K_{IR}2.1$ proteins in response to propafenone. (**A**) $K_{IR}2.1$ expression of cells after being treated with different concentrations of propafenone (1, 10, 25, and 50 μM) for 24 h ($n = 5$). (**B**) Summarized results of $K_{IR}2.1$ expression in control and cells treated for propafenone ($n = 5$). The control protein level was set at 1 after correction for loading. Non-transfected cells (NT) were used as a negative control. Ponceau staining was used as a loading control. * $p < 0.05$, ** $p < 0.01$, *** $p < 0.001$ vs. control of propafenone.

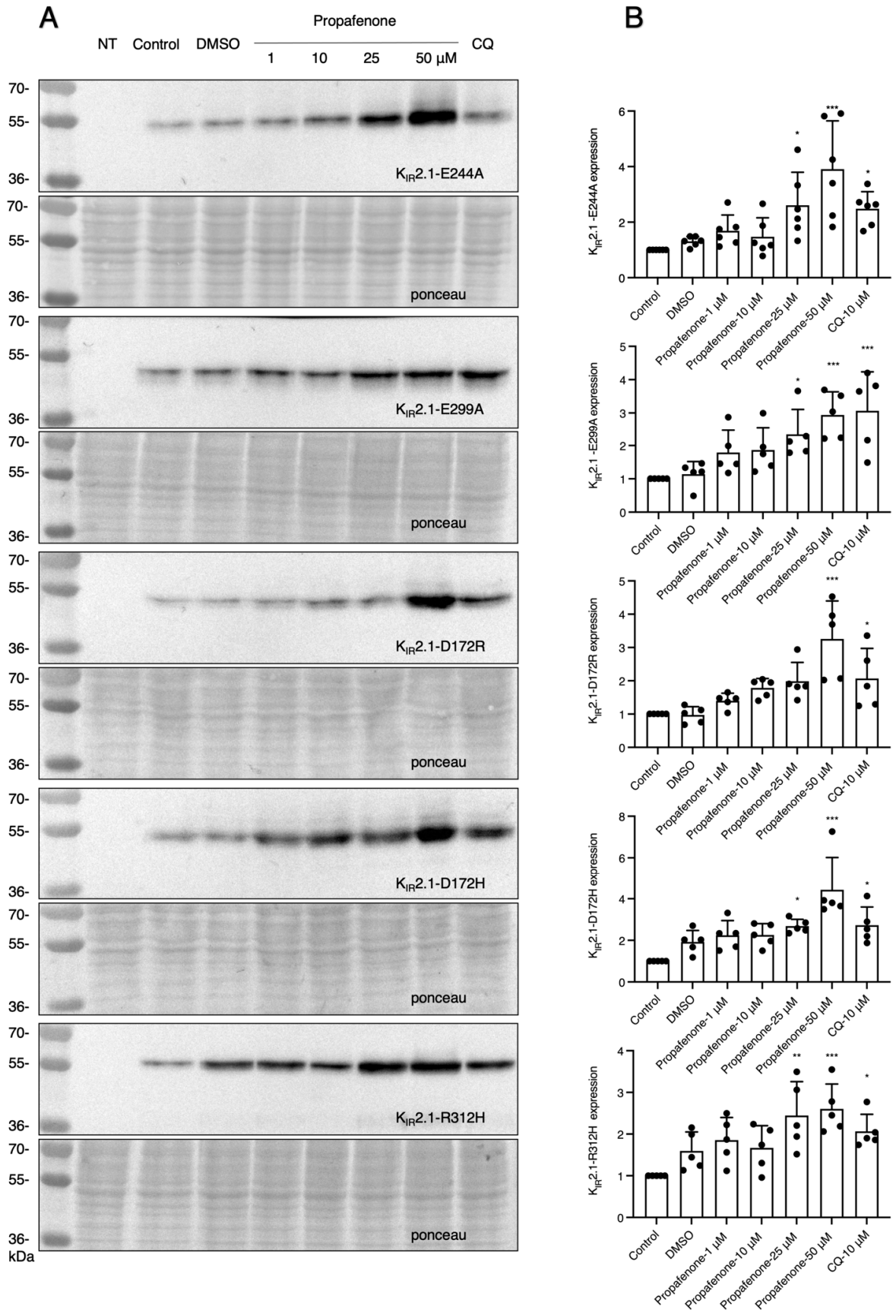

Figure 5. Mutations of polyamine binding sites and the drug-channel binding location do not interfere with the chronic effect of propafenone on $K_{IR}2.1$ protein expression. (**A**) $K_{IR}2.1$ expression of cells after

treatment with increasing concentrations of propafenone in different mutant $K_{IR}2.1$ proteins (D172R (n = 5), D172H (n = 5), E244A (n = 6), E299A (n = 5), and R312H (n = 5)). Cells were treated with different concentrations of propafenone (1, 10, 25, 50 and μM) for 24 h. (**B**) Summarized results of $K_{IR}2.1$ expression levels in control and cells treated for propafenone (n = 5 or 6). The control protein level was set at 1 after correction for loading. Non-transfected cells (NT) were used as a negative control. Ponceau staining was used as a loading control. * $p < 0.05$, ** $p < 0.01$, *** $p < 0.001$ vs. control.

2.4. $K_{IR}2.1$-GFP/Dendra2 Clustering and Protein Turnover Rate Indicate That Propafenone May Interfere in Late Endosome Function

Live imaging showed that propafenone and chloroquine (CQ) can both cause intracellular $K_{IR}2.1$ accumulation but in a different pattern (Figure 6A). CQ causes scattered clusters of $K_{IR}2.1$ on the edge of the cell, while propafenone causes brighter clusters both in the edge and center of the cell at 50 μM, but not at 10 μM. As shown before, CQ increases the expression of $K_{IR}2.1$ protein by inhibiting its degradation via the lysosomal pathway [36]. The different appearance of clusters in response to propafenone may point to a different mechanism for cell trafficking in comparison to CQ.

CHO-KD cells were used to investigate whether propafenone's long-term effect is late endosome/lysosome-related. $K_{IR}2.1$-Dendra2 is present in round clusters in the interior of the cells, which accumulate inside cells upon administration of 25 μM propafenone (3–48 h) (Figure 6B). Images of DMSO-treated cells (Figure 6B) show that $K_{IR}2.1$-Dendra2 is present in the plasma membrane and the cell's interior as many little clusters. Time-lapse imaging (Video S1, CHO-KD cells treated with DMSO) shows that these clusters move fast in all directions. $K_{IR}2.1$-Dendra2 moves slower after being treated with propafenone, and big clusters appeared in the cells' interiors (Video S1). The number of small clusters decreased (Video S1, CHO-KD cells treated with 25 μM propafenone for 3 h, 6 h, 24 h, and 48 h), and more and larger clusters became visible in the cells. Video S1 shows that the larger clusters of $K_{IR}2.1$-Dendra2 display less movement, while the remaining small clusters move faster. For the cells treated for 48 h with propafenone, multivesicular bodies (MVBs) appeared among the clusters of proteins (Figure 6B, enlarged picture), indicating that $K_{IR}2.1$-Dendra2 might accumulate in late endosome-like structures. Similarly, as seen for protein expression levels (Figure 5), intracellular $K_{IR}2.1$ protein accumulation was independent of D172H, D172R, E244A, E299A, or R312H mutations (Figure 6C).

MVBs will deliver cargo destined for degradation to the lysosome [41,42]. Therefore, we tested the half-life of the $K_{IR}2.1$ proteins in HEK-KWGF cells in the presence of the translation inhibitor cycloheximide (CHX) (200 μg/mL). In the CQ treated group, the $T_{1/2}$ was significantly increased compared to the control ($T_{1/2}$ = 9.494 h vs. 4.774 h, Figure 7C,D). In contrast, no significant difference in $T_{1/2}$ was found following propafenone treatment ($T_{1/2}$ of 4.774 h in the control group vs. 5.247 h after propafenone treatment) (Figure 7A,B). Thus, propafenone does not impair the degradation of $K_{IR}2.1$ proteins in lysosomes.

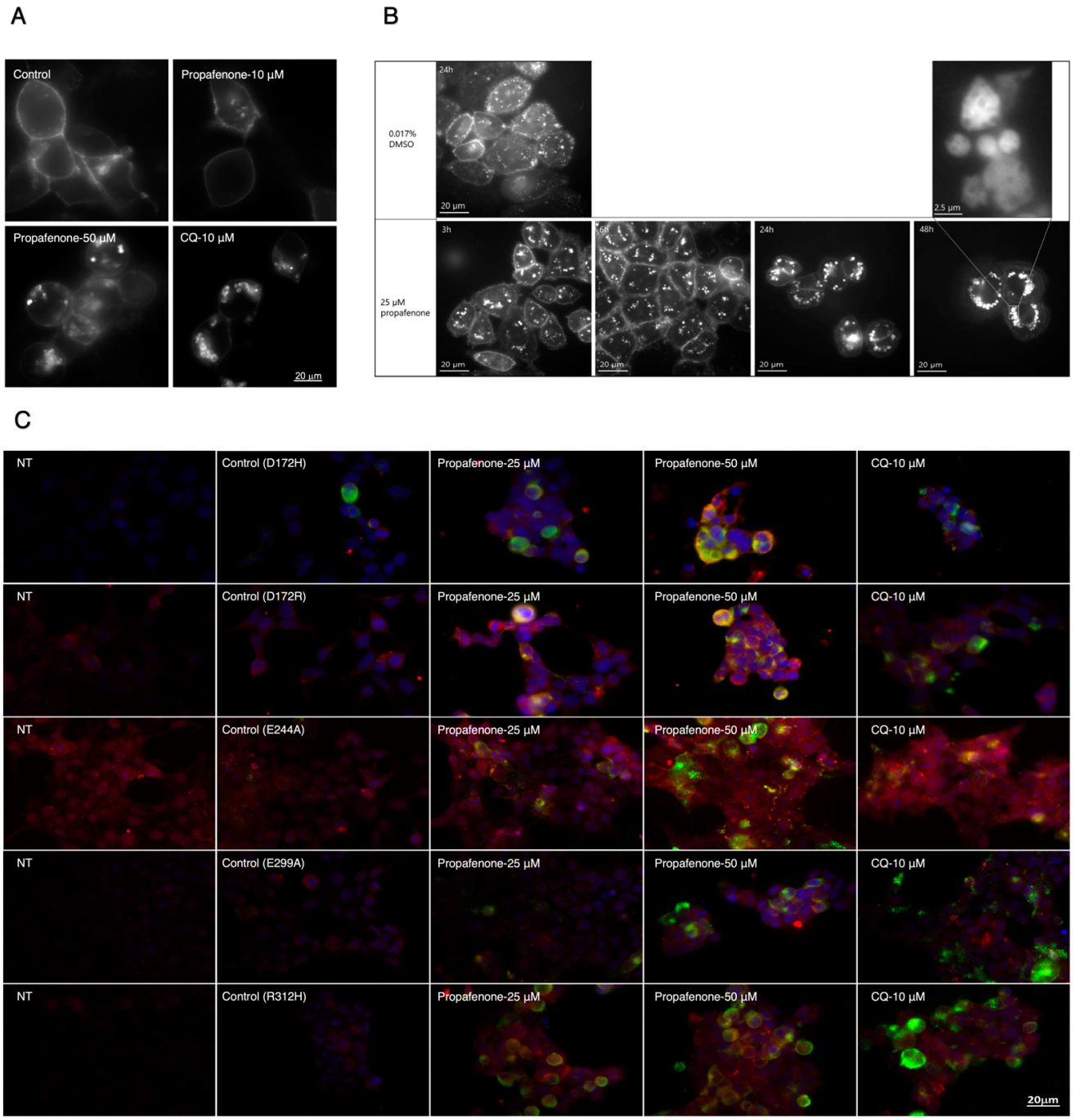

Figure 6. Propafenone induces $K_{IR}2.1$ protein clustering in HEK-KWGF cells, CHO-KD cells, and HEK293 cells. (**A**) Propafenone (10, 50 µM, 24 h) induced intracellular accumulation of WT and mutant $K_{IR}2.1$ proteins in HEK-KWGF cells. 488 nm laser light was used to visualize $K_{IR}2.1$-GFP. The scale bar indicates 20 µm. (**B**) Cloned CHO-KD cells were incubated for 24 h with DMSO or propafenone at 25 µM for different periods (3, 6, 24, or 48 h). Images were taken at 60 x magnification. 488 nm laser light was used to visualize $K_{IR}2.1$-Dendra2. The scale bar indicates 20 µm. (**C**) Subcellular localization of D172R, D172H, E244A, E299A, and R312H $K_{IR}2.1$ proteins in HEK293 cells. Cells were treated with different concentrations of propafenone (25, 50 µM) for 24 h. Non-transfected cells (NT) were used as a negative control. Propafenone and CQ treatment induce $K_{IR}2.1$ protein accumulation. $K_{IR}2.1$ was detected by specific antibodies (green) Cadherin (membrane staining) by Pan-Cadherin antibodies (red). The nuclei were stained with DAPI (blue). The scale bar indicates 20 µm.

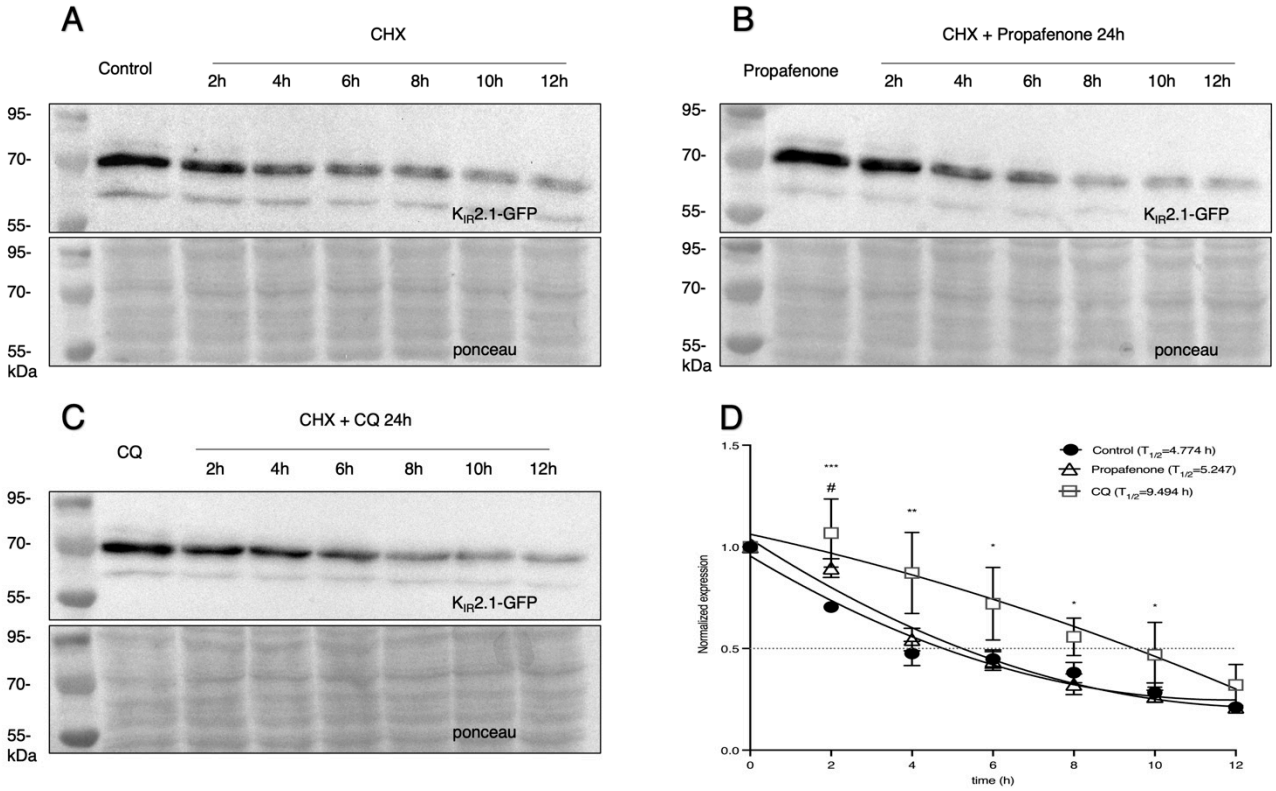

Figure 7. Cycloheximide (CHX) assay of K_{IR}2.1 degradation in HEK-KWGF cells. (**A**) Example of K_{IR}2.1 protein degradation after exposure to 200 μg/mL CHX for different time intervals. (**B**) Example of K_{IR}2.1 protein degradation in cells that were treated with propafenone for 24 h. 200 μg/mL CHX was added for different time periods before lysates were prepared at t = 24 h. (**C**) Example of K_{IR}2.1 protein degradation in cells that were treated with CQ for 24 h. 200 μg/mL CHX was added for different time periods before lysates were prepared at t = 24 h. (**D**) Quantification of CHX assays to depict normalized K_{IR}2.1 expression vs. timed CHX treatment with or without propafenone or CQ treatment (n = 5). The dotted line indicates 50% of the initial normalized K_{IR}2.1 protein signal. * indicates $p < 0.05$, ** indicates $p < 0.01$ *** indicates $p < 0.001$ when CQ vs. control. # indicates $p < 0.05$ when comparing propafenone vs. control. To show the declining trend of protein expression after exposure to 200 μg/mL CHX, the loading protein in Figure (**A**) was twice that of Figure (**B**) and Figure (**C**).

3. Discussion

We confirmed that acute administration of propafenone at low concentrations increases K_{IR}2.1 currents in HEK-KWGF cells, which is similar to the results obtained in CHO cells transiently transfected with WT K_{IR}2.1 [30]. Therefore, propafenone was shown to act as a K_{IR}2.1 agonist, which we named "Agokir" [29]. However, since the effect of propafenone on K_{IR}2.1 carried current is acute, chronic treatment will be required for long-term IK_1 enhancement. Therefore, we investigated propafenone's long-term effect on K_{IR}2.1 channels.

Propafenone is commonly administered in the clinic to treat atrial fibrillation because of its sodium channel blocking activity [43,44]. This sodium channel blocking property results in a markedly depressed depolarization phase of the action potential and a widening of the QRS complex [45–47]. Some studies also showed that QRS duration was increased with or without QT interval prolongation in humans after treatment with propafenone [48–52]. Therapeutic plasma levels of propafenone in humans were estimated to range from 0.53 to 5.28 μM [33,53,54]. Furthermore, propafenone concentrations in human atrial tissues were on average ten times higher than those found in the plasma [53]. Such concentrations

approach or are even similar to the concentrations found in our work, in which the chronic effect on $K_{IR}2.1$ protein results in an increase in expression levels.

In the present work, propafenone increases the outward component acutely at low concentrations (0.5 and 1 μM). Such an increase was shown to be achieved by the propafenone-$K_{IR}2.1$ channel binding-mediated decrease of channel affinity for polyamines and thus current rectification [30]. In contrast, propafenone at higher concentrations (25 and 50 μM) shows a strong acute blocking effect on both the inward and outward components. This block is caused by a propafenone-mediated decrease of the negative charge of the channel pore and channel affinity for phosphatidylinositol 4,5-bisphosphate (PIP_2), which is a lipid critical for channel activation [12,43]. For the long-term effect, however, propafenone treatment at high concentrations results in a significant increase in IK_1 densities. These latter electrophysiological measurements were performed in the absence of propafenone, thereby excluding its acute effect on $K_{IR}2.1$ channels. This significant increase likely occurred because propafenone inhibits channel backward trafficking, thereby indirectly increasing the $K_{IR}2.1$ channel expression level on the cell membrane.

In order to test propafenone's specificity for increasing $K_{IR}2.1$ channel expression, we investigated its effects on hERG channel expression, which is a voltage-gated potassium channel and thereby different from the non-voltage-gated $K_{IR}2.1$ channel. Sodium channel expression was also tested because propafenone is used as its blocking agent in the clinic [33,55]. Propafenone did not interfere with the expression levels of these two channels, revealing that propafenone has at least some specificity towards K_{IR} channels. Some studies showed that there is reciprocal regulation between $Na_v1.5$ and $K_{IR}2.1$ channels [56–62]. $K_{IR}2.1$ overexpression increases the expression levels of $Na_v1.5$ in mouse hearts [58]. As propafenone increases the expression level of $K_{IR}2.1$ proteins significantly but does not interfere with that of $Na_v1.5$ in the same cells and with the same treatment in our study. We may thus hypothesize that propafenone might either affect cooperation between the two channels or act on a part of the trafficking pathway in which both channels do not cooperate. The previous study also showed that $Na_v1.5$ protein reduces $K_{IR}2.1$ protein internalization and promote its presence at the cell surface [58]. As the expression level of $Na_v1.5$ was not changed, the increased expression of $K_{IR}2.1$ protein was only affected by propafenone.

Ba^{2+} is an efficient IK_1 blocking ion [10,63]. The atomic radius of Ba^{2+} is close to that of K^+; therefore, it will fit into the K^+ selectivity filter and remain in that position due to its larger charge, effectively blocking the inward and outward K^+ flow [64–66]. At the same time, we also investigated a non-conducting $K_{IR}2.1$-AAA mutant to test the influence of channel functions on the long-term effect of propafenone. The results showed that the expression of $K_{IR}2.1$ channel proteins displayed no significant differences when compared with WT or not inhibited channels, which suggests that channel function (i.e., K^+ conduction) is not involved in the long-term effect of propafenone.

Polyamines, responsible for naturally occurring inward rectification, occupy two positions in the $K_{IR}2.x$ channels: the cytoplasmic pore domain at $K_{IR}2.1$ E224 and E299 and the transmembrane pore domain at D172 [2,22]. Western blotting pointed out that propafenone dose-dependently increases WT, E224A, E299A, D172H, and D172R-$K_{IR}2.1$ protein expression in HEK-293 cells. Therefore, polyamine binding sites, and most likely polyamine binding too, appear not to be involved in the propafenone-mediated increase in $K_{IR}2.1$ expression levels.

Dynamics simulations predicted that propafenone interacts with $K_{IR}2.1$ by forming a hydrogen bond with the cysteine residue C311, which is identified as a direct channel-drug binding site [29,30,67,68]. Because of the proximity of C311 to the R312 residue [69], it is possible that the mutation R312H allosterically modifies the 310-QCRSSY-315 C-terminus domain, thereby precluding propafenone channel interaction. Increased $K_{IR}2.1$-R312H expression showed a similar result as WT, revealing that drug-channel interaction is most likely not involved in the chronic response to propafenone. In conclusion, propafenone

specifically works on $K_{IR}2$ channels, but neither K^+ conduction, polyamine binding sites, nor direct drug-channel interactions are involved in the long-term effects of propafenone.

HEK-KWGF cells showed an intracellular accumulation of $K_{IR}2.1$ proteins after being treated with propafenone. The intracellular patterns, however (Figure 6A), were distinct from cells treated with CQ, which is known to inhibit lysosomes. A potential explanation for this difference is that propafenone acts on both late endosomes and lysosomes, or on endosomes only. Live imaging on CHO-KD cells supported the observations reported above and revealed that after incubating 25 μM of propafenone for only 3 h, $K_{IR}2.1$-Dendra2 proteins started to accumulate in the cytoplasm (Figure 6B). More and bigger clusters appeared at the following time points. The large clusters of $K_{IR}2.1$-Dendra2 proteins show less movement, which is in line with earlier research in which lysosomal diameter was increased using sucrose; enlarged lysosomes were correlated to a reduced diffusion rate [70]. Furthermore, MVBs were shown in the protein clusters after 48 h of incubation with propafenone, indicating that $K_{IR}2.1$-Dendra2 may accumulate within the late endosome compartment [71]. Protein also accumulates in late endosomes when lysosomes do not function well [71,72]. However, propafenone treatment did not increase $T_{1/2}$ as CQ, indicating that propafenone does not inhibit the function of lysosomes per se. From all these results, we conclude that chronic propafenone treatment increases $K_{IR}2.1$ protein expression and $K_{IR}2.1$ current densities in vitro following a 24 h treatment, which persists after washout and is potentially associated with pre-lysosomal trafficking inhibition. Moreover, additional proteins following a similar degradation route as $K_{IR}2.1$ could be affected similarly to propafenone.

Our data shows that propafenone can function as AgoKir at low concentrations without disturbing $K_{IR}2.1$ protein handling; however, it also shows long-term effects at higher concentrations. It is worthwhile to search for more potent propafenone analogs that should increase IK_1 without affecting $K_{IR}2.1$ channel expression, thus contributing to the development of new therapeutic avenues to address diseases related to dysfunctional $K_{IR}2.1$.

4. Materials and Methods

4.1. Cell Culture

Cell lines were cultured in Dulbecco's Modified Eagles Medium (DMEM; Lonza, Breda, The Netherlands) supplemented with 10% fetal bovine serum (FBS; Sigma-Aldrich, St. Louis, MO, USA), 200 mM L-glutamine (Lonza), and 10.000 U/mL penicillin-streptomycin (Lonza) at 37 °C with 5% CO_2. These cells contain human embryonic kidney (HEK)-293 cells (ATCC, Accession Number: CRL-1573), HEK-KWGF cells [73] (HEK cells stably expressing C-terminal GFP-tagged murine $K_{IR}2.1$), CHO-KD cells [74] (Chinese Hamster Ovary cells stably expressing Dendra-2-tagged $K_{IR}2.1$), HEK-hERG cells [75] (cells stably expressing human hERG), and HEK-$Na_v1.5$ cells [75] (HEK cells stably expressing both $K_{IR}2.1$ and human sodium channels ($Na_v1.5$)). Cells for each time point were seeded on the same day, and drugs were added for the indicated time before the harvest of all samples. Cell confluency at the time of processing was 80–90%, 50–60%, and 10% for biochemical, (immuno)fluorescent, and patch-clamp electrophysiology experiments, respectively.

4.2. $K_{IR}2.1$-Mutant Expression Constructs and Transfection

$K_{IR}2.1$-E224A and E299A mutant constructs were obtained from Dr. Tristani-Firouzi (University of Utah School of Medicine, USA), and functional characteristics have been described previously by others [76] and us [34,77]. $K_{IR}2.1$-D172R and D172H mutant constructs were obtained from Dr. So (Seoul National University, College of Medicine, Republic of Korea), and functional characteristics have been described before [78]. A $K_{IR}2.1$-R312H mutant construct was obtained from Dr. Bendahhou (Université Côte d'Azur, France), and functional characteristics have been described recently [79]. Cell transfection was performed with linear polyethylenimine (PEI) with a molecular weight of 25,000 (Polysciences, Hirschberg an der Bergstrasse, Germany) as described previously by

us [80] and references therein. Transfection efficacies were 30–70% and routinely checked by GFP transfection.

4.3. Drugs

Chloroquine (CQ) (Sigma, St. Louis, MO, United States, cat. No. C6628) was dissolved in sterile water at a concentration of 10 mM and stored at −20 °C. Propafenone (Sigma, cat. No. C7698) was dissolved in DMSO at a concentration of 100 mM and stored at −20 °C until use. Cycloheximide (CHX, Sigma, cat. No. C7698) was dissolved in sterile water at a concentration of 5 mg/mL, stored, and aliquoted at −20 °C until use. All drugs were diluted on the day they were used.

4.4. Western Blot

Cell lysates were prepared in Buffer D (20 mM HEPES, 125 mM NaCl, 10% glycerol, 1 mM EGTA, 1 mM dithiothreitol, 1 mM EDTA, and 1% Triton X-100 (pH 7.6)) supplemented with 0.2 mM phenylmethylsulfonyl fluoride (PMSF) and 4 $\mu g \cdot mL^{-1}$ aprotinin. Protein lysate (30 or 60 µg) was separated by 7% or 10% SDS-PAGE and blotted onto a nitrocellulose membrane (Bio-Rad Laboratories, Veenendaal, The Netherlands). Ponceau staining was used as a loading control for subsequent quantification. Blots were blocked for 1 h with 5% Protifar dissolved in Tris-buffered saline/Tween 20 (20 mM Tris-HCl (pH 8.0), 150 mM NaCl, 0.05% (*v*/*v*) Tween-20). For protein detection, the membrane was incubated with anti-K_{IR}2.1 (1:1000; Sigma-Aldrich, St. Louis, MO, USA), anti-GFP (1:500; Santa Cruz Biotechnology, Heidelberg, Germany), anti-hERG (1:2500; Alomone Labs, Jerusalem, Israel), or anti-sodium channel primary antibody (1:2000; custom-made [81]). A peroxidase-conjugated Goat anti-Mouse (Jackson ImmunoResearch, West Grove, PA, USA) or Goat anti-Rabbit (Jackson ImmunoResearch, West Grove, PA, USA) antibody was applied as the second primary antibody. Final detection was performed using the Standard ECL procedure (Amersham Bioscience, Buckinghamshire, UK). Quantification was done by Image Lab software version 6.1 (Bio-Rad Laboratories, Veenendaal, The Netherlands).

4.5. Cloning

CHO-KD single-cell suspension was counted in a Brand™ Bürker counting chamber (Fisher Scientific, Landsmeer, The Netherlands). The cell suspension was diluted to obtain a concentration of 10 cells per mL, and cells were cultured in 96-well plates (100 µL/well). Cells were examined under a Nikon TMS inverted microscope (Nikon Instruments Europe B.V., Amsterdam, The Netherlands) after forming a single clone. The clones were expanded and then imaged by a Nikon Eclipse 80i epifluorescence microscope (Nikon Instruments Europe B.V.).

4.6. Live Imaging with Confocal Microscopy

HEK-KWGF cells were treated with propafenone (10, 50 µM) for 24 h, and then 488 nm laser light was used to visualize K_{IR}2.1-GFP. We cloned the existing CHO-KD cell line to create a pool of cells with high K_{IR}2.1-Dendra2 expression. CHO-KD cells were treated with propafenone at 25 µM for different time courses (3, 6, 24, and 48 h). Then they were placed under a Nikon Eclipse Ti2-E inverted microscope (Nikon Instruments Europe B.V.) equipped with a ×60 oil immersion objective (numerical aperture 1.49; CAIRN research, Faversham, United Kingdom) at room temperature. The laser light at 488 nm was used to visualize K_{IR}2.1–Dendra2. For 20 min, a photo was taken every 20 s. Movie Maker (Microsoft, 2012) was used to make a time-lapse of 60 images.

4.7. Immunofluorescence Microscopy

HEK-293 cells were cultured on Ø 15 mm glass coverslips coated with 0.1% gelatin. Different K_{IR}2.1 mutant expression constructs (E224A, E299A, D172R, D172H, and R312H) were transfected into HEK-293 for 24 h using PEI before the cells were treated with propafenone (25, 50 µM) or CQ (10 µM) for 24 h. Then the coverslips were washed

with PBS, fixated with 3%-paraformaldehyde, permeabilized with 0.5% Triton X-100 (in PBS), quenched with PBS/glycine (50 mM), and incubated twice with NET-gel (0.25% gelatin, 50 mM Tris-Cl, 150 mM NaCl, 4 mM EDTA, 0.05% Igepal, ± 0.01% NaN_3, pH 7.4). Primary antibodies used were $K_{IR}2.1$ (1:400; Sigma-Aldrich, St. Louis, MO, USA) and Pan-Cadherin (1:800; Sigma-Aldrich, St. Louis, MO, USA). After the cells were washed, they were incubated with secondary antibodies: goat anti-mouse (Green, 1:100; Jackson ImmunoResearch Laboratories Inc., West Grove, PA, USA) and donkey anti-rabbit (Alexa Red, 1:350; Jackson ImmunoResearch Laboratories Inc.). Cell nuclei were stained with 4′,6-diamidino-2-phenylindole (DAPI; 1:100; Molecular Probes, Leiden, The Netherlands). Coverslips were mounted with Vectashield (Vector Laboratories Inc., Burlingame, CA, USA) and imaged using a Nikon Eclipse 80i (Nikon, Amsterdam, The Netherlands) and NIS elements Basic Research (Nikon, Amsterdam, The Netherlands) software.

4.8. Washout Experiment

HEK-KWGF cells were seeded in Ø 60 mm dishes overnight. 24 h after treatment with propafenone (25 or 50 μM), the medium of the cells was replaced by fresh supplemented DMEM. Protein lysates were harvested 24 or 48 h after changing the medium. The $K_{IR}2.1$ expression level was detected by Western blot.

4.9. Cycloheximide Assay

HEK-KWGF cells were seeded in Ø 35 mm dishes. After 24 h, cells were left untreated (control) or treated with 50 μM propafenone or 10 μM CQ for 24 h. 200 μg/mL cycloheximide was added during the last phases (2, 4, 6, 8, 10, or 12 h) of the 24 h treatment period. Cell lysates were prepared and processed as indicated in Section 4.4. Since propafenone and CQ increased the expression levels of $K_{IR}2.1$-GFP protein compared to control conditions before the start of CHX application, twice the amount of control lysate loaded on SDS-PAGE to enable visualization of the $K_{IR}2.1$ protein under control conditions at CHX t = 10 and t = 12 using similar ECL exposure times as for propafenone and CQ conditions.

4.10. Patch Clamp Electrophysiology

Whole-cell clamp measurements were performed using an AxoPatch 200B amplifier controlled by pClamp10.4 software (Molecular Devices, LLC, San Jose, CA, USA). The $K_{IR}2.1$ current in HEK-KWGF cells was measured at room temperature. Patch pipettes were made with a Sutter P-2000 puller (HEKA Elektronik, Lambrecht, Germany) and had resistances of 1–3 MΩ.

HEK-KWGF cells were grown on 0.1% gelatin (Bio-Rad, Veenendaal, The Netherlands), coated Ø 12-mm coverslips in a 12-well plate. For acute effect, after taking baseline measurements, the cells were perfused for 5 min with propafenone (0.5, 1, and 25 μM), followed by a 5-min washout. For the chronic effect, cells were randomly divided into two groups, the treatment groups were treated with 50 μM of propafenone for 24 h, while the control group did not undergo any treatment. To record $K_{IR}2.1$ currents, voltage-clamp measurements were performed by applying 1s test pulses ranging between −120 and +30 mV with 10 mV increments. Extracellular solution for whole-cell $I_{KIR2.1}$ measurements contained (in mmol/L): NaCl 140, KCl 5.4, $CaCl_2$ 1, $MgCl_2$ 1, glucose 6, $NaHCO_3$ 17.5, HEPES 15, pH 7.4/NaOH. The pipette solution contained (in mmol/L) potassium gluconate 125, KCl 10, HEPES 5, EGTA 5, $MgCl_2$ 2, $CaCl_2$ 0.6, Na2ATP 4, pH 7.20/KOH.

4.11. Statistics

Data are expressed as mean ± S.D. Differences between group averages were tested using a one-way ANOVA with a post-hoc test (Tukey's HSD), or an unpaired *T*-test. Data were considered significant when the *p*-value was less than 0.05. Statistical analysis was performed using GraphPad Prism version 9 (GraphPad Software, San Diego, CA, USA).

Supplementary Materials: The following supporting information can be downloaded at: https://www.mdpi.com/article/10.3390/ph16030404/s1, Figure S1: Acute effect of propafenone; Video S1: Propafenone time-dependently induces K_{IR}2.1-Dendra2 clustering in CHO-KD cells.

Author Contributions: Conceptualization, M.A.G.v.d.H.; methodology, E.L., L.W., and W.K.; writing—original draft preparation, E.L.; writing—review and editing, M.A.G.v.d.H.; supervision, M.A.G.v.d.H.; project administration, M.A.G.v.d.H.; funding acquisition, E.L. All authors have read and agreed to the published version of the manuscript.

Funding: EL was supported by the Chinese Scholarship Council.

Institutional Review Board Statement: Not applicable.

Informed Consent Statement: Not applicable.

Data Availability Statement: All the research data are available in article and the supporting information section.

Acknowledgments: We are grateful for the sodium channel antibody obtained from Peter Mohler. We thank Tristani-Firouzi, So, and Bendahhou for providing the mutant K_{IR}2.1 expression constructs as described in Section 4.2.

Conflicts of Interest: The authors declare no conflict of interest.

References

1. Kurata, H.T.; Phillips, L.R.; Rose, T.; Loussouarn, G.; Herlitze, S.; Fritzenschaft, H.; Enkvetchakul, D.; Nichols, C.G.; Baukrowitz, T. Molecular basis of inward rectification: Polyamine interaction sites located by combined channel and ligand mutagenesis. *J. Gen. Physiol.* **2004**, *124*, 541–554. [CrossRef]
2. Hibino, H.; Inanobe, A.; Furutani, K.; Murakami, S.; Findlay, I.; Kurachi, Y. Inwardly rectifying potassium channels: Their structure, function, and physiological roles. *Physiol. Rev.* **2010**, *90*, 291–366. [CrossRef]
3. Tao, X.; Avalos, J.L.; Chen, J.; MacKinnon, R. Crystal structure of the eukaryotic strong inward-rectifier K^+ channel Kir2.2 at 3.1 A resolution. *Science* **2009**, *326*, 1668–1674. [CrossRef] [PubMed]
4. Anumonwo, J.M.; Lopatin, A.N. Cardiac strong inward rectifier potassium channels. *J. Mol. Cell. Cardiol.* **2010**, *48*, 45–54. [CrossRef] [PubMed]
5. Kubo, Y.; Baldwin, T.J.; Jan, Y.N.; Jan, L.Y. Primary structure and functional expression of a mouse inward rectifier potassium channel. *Nature* **1993**, *362*, 127–133. [CrossRef]
6. Lopatin, A.N.; Makhina, E.N.; Nichols, C.G. Potassium channel block by cytoplasmic polyamines as the mechanism of intrinsic rectification. *Nature* **1994**, *372*, 366–369. [CrossRef]
7. Ficker, E.; Taglialatela, M.; Wible, B.A.; Henley, C.M.; Brown, A.M. Spermine and spermidine as gating molecules for inward rectifier K^+ channels. *Science* **1994**, *266*, 1068–1072. [CrossRef] [PubMed]
8. Nakamura, T.Y.; Artman, M.; Rudy, B.; Coetzee, W.A. Inhibition of rat ventricular IK1 with antisense oligonucleotides targeted to Kir2.1 mRNA. *Am. J. Physiol.* **1998**, *274*, H892–H900. [CrossRef] [PubMed]
9. Lange, P.S.; Er, F.; Gassanov, N.; Hoppe, U.C. Andersen mutations of KCNJ2 suppress the native inward rectifier current IK1 in a dominant-negative fashion. *Cardiovasc. Res.* **2003**, *59*, 321–327. [CrossRef] [PubMed]
10. Iijima, A.; Svecova, O.; Hosek, J.; Kula, R.; Bebarova, M. Sildenafil affects the human Kir2.1 and Kir2.2 channels at clinically relevant concentrations: Inhibition potentiated by low Ba^{2+}. *Front. Pharmacol.* **2023**, *14*, 1136272. [CrossRef]
11. Mylona, P.; Gokhale, D.A.; Taylor, G.M.; Sibley, C.P. Detection of a high-frequency silent polymorphism (C→T) in the kir2.1 (KCNJ2) inwardly rectifying potassium channel gene by polymerase chain reaction and single strand conformation polymorphism. *Mol. Cell. Probes* **1998**, *12*, 331–333. [CrossRef] [PubMed]
12. Zaritsky, J.J.; Redell, J.B.; Tempel, B.L.; Schwarz, T.L. The consequences of disrupting cardiac inwardly rectifying K^+ current (I(K1)) as revealed by the targeted deletion of the murine Kir2.1 and Kir2.2 genes. *J. Physiol.* **2001**, *533*, 697–710. [CrossRef]
13. Dhamoon, A.S.; Jalife, J. The inward rectifier current (IK1) controls cardiac excitability and is involved in arrhythmogenesis. *Heart Rhythm* **2005**, *2*, 316–324. [CrossRef]
14. Reilly, L.; Eckhardt, L.L. Cardiac potassium inward rectifier Kir2: Review of structure, regulation, pharmacology, and arrhythmogenesis. *Heart Rhythm* **2021**, *18*, 1423–1434. [CrossRef]
15. Liu, Q.; Sun, J.; Dong, Y.; Li, P.; Wang, J.; Wang, Y.; Xu, Y.; Tian, X.; Wu, B.; He, P.; et al. Tetramisole is a new I(K1) channel agonist and exerts I(K1) -dependent cardioprotective effects in rats. *Pharmacol. Res. Perspect.* **2022**, *10*, e00992. [CrossRef] [PubMed]
16. Weaver, C.D.; Denton, J.S. Next-generation inward rectifier potassium channel modulators: Discovery and molecular pharmacology. *Am. J. Physiol. Cell. Physiol.* **2021**, *320*, C1125–C1140. [CrossRef] [PubMed]
17. van der Heyden, M.A.; Sanchez-Chapula, J.A. Toward specific cardiac I(K1) modulators for in vivo application: Old drugs point the way. *Heart Rhythm* **2011**, *8*, 1076–1080. [CrossRef]

18. Fakler, B.; Brandle, U.; Glowatzki, E.; Weidemann, S.; Zenner, H.P.; Ruppersberg, J.P. Strong voltage-dependent inward rectification of inward rectifier K^+ channels is caused by intracellular spermine. *Cell* **1995**, *80*, 149–154. [CrossRef]
19. Baronas, V.A.; Kurata, H.T. Inward rectifiers and their regulation by endogenous polyamines. *Front. Physiol.* **2014**, *5*, 325. [CrossRef]
20. Yang, J.; Jan, Y.N.; Jan, L.Y. Control of rectification and permeation by residues in two distinct domains in an inward rectifier K^+ channel. *Neuron* **1995**, *14*, 1047–1054. [CrossRef]
21. Xie, L.H.; John, S.A.; Weiss, J.N. Inward rectification by polyamines in mouse Kir2.1 channels: Synergy between blocking components. *J. Physiol.* **2003**, *550*, 67–82. [CrossRef] [PubMed]
22. Nichols, C.G.; Lee, S.J. Polyamines and potassium channels: A 25-year romance. *J. Biol. Chem.* **2018**, *293*, 18779–18788. [CrossRef] [PubMed]
23. Xia, M.; Jin, Q.; Bendahhou, S.; He, Y.; Larroque, M.M.; Chen, Y.; Zhou, Q.; Yang, Y.; Liu, Y.; Liu, B.; et al. A Kir2.1 gain-of-function mutation underlies familial atrial fibrillation. *Biochem. Biophys. Res. Commun.* **2005**, *332*, 1012–1019. [CrossRef] [PubMed]
24. Yim, J.; Kim, K.B.; Kim, M.; Lee, G.D.; Kim, M. Andersen-Tawil Syndrome With Novel Mutation in KCNJ2: Case Report. *Front. Pediatr.* **2021**, *9*, 790075. [CrossRef]
25. Le Tanno, P.; Folacci, M.; Revilloud, J.; Faivre, L.; Laurent, G.; Pinson, L.; Amedro, P.; Millat, G.; Janin, A.; Vivaudou, M.; et al. Characterization of Loss-Of-Function KCNJ2 Mutations in Atypical Andersen Tawil Syndrome. *Front. Genet.* **2021**, *12*, 773177. [CrossRef]
26. Marrus, S.B.; Cuculich, P.S.; Wang, W.; Nerbonne, J.M. Characterization of a novel, dominant negative KCNJ2 mutation associated with Andersen-Tawil syndrome. *Channels* **2011**, *5*, 500–509. [CrossRef]
27. Vivekanandam, V.; Mannikko, R.; Skorupinska, I.; Germain, L.; Gray, B.; Wedderburn, S.; Kozyra, D.; Sud, R.; James, N.; Holmes, S.; et al. Andersen-Tawil syndrome: Deep phenotyping reveals significant cardiac and neuromuscular morbidity. *Brain* **2022**, *145*, 2108–2120. [CrossRef]
28. Miake, J.; Marban, E.; Nuss, H.B. Functional role of inward rectifier current in heart probed by Kir2.1 overexpression and dominant-negative suppression. *J. Clin. Investig.* **2003**, *111*, 1529–1536. [CrossRef]
29. Van der Schoor, L.; Van Hattum, E.J.; de Wilde, S.M.; Harlianto, N.I.; Van Weert, A.J.; Bloothooft, M.; Van der Heyden, M.A.G. Towards the Development of AgoKirs: New Pharmacological Activators to Study Kir2.x Channel and Target Cardiac Disease. *Int. J. Mol. Sci.* **2020**, *21*, 5746. [CrossRef]
30. Gomez, R.; Caballero, R.; Barana, A.; Amoros, I.; De Palm, S.H.; Matamoros, M.; Nunez, M.; Perez-Hernandez, M.; Iriepa, I.; Tamargo, J.; et al. Structural basis of drugs that increase cardiac inward rectifier Kir2.1 currents. *Cardiovasc. Res.* **2014**, *104*, 337–346. [CrossRef]
31. Stoschitzky, K.; Stoschitzky, G.; Lercher, P.; Brussee, H.; Lamprecht, G.; Lindner, W. Propafenone shows class Ic and class II antiarrhythmic effects. *Europace* **2016**, *18*, 568–571. [CrossRef] [PubMed]
32. Kovacs, B.; Yakupoglu, H.Y.; Eriksson, U.; Krasniqi, N.; Duru, F. Medical therapy with flecainide and propafenone in atrial fibrillation: Long-term clinical experience in the tertiary care setting. *Cardiol. J.* **2023**, *30*, 82–90. [CrossRef] [PubMed]
33. Bryson, H.M.; Palmer, K.J.; Langtry, H.D.; Fitton, A. Propafenone. A reappraisal of its pharmacology, pharmacokinetics and therapeutic use in cardiac arrhythmias. *Drugs* **1993**, *45*, 85–130. [CrossRef]
34. Takanari, H.; Nalos, L.; Stary-Weinzinger, A.; de Git, K.C.; Varkevisser, R.; Linder, T.; Houtman, M.J.; Peschar, M.; de Boer, T.P.; Tidwell, R.R.; et al. Efficient and specific cardiac IK(1) inhibition by a new pentamidine analogue. *Cardiovasc. Res.* **2013**, *99*, 203–214. [CrossRef] [PubMed]
35. de Git, K.C.; de Boer, T.P.; Vos, M.A.; Van der Heyden, M.A.G. Cardiac ion channel trafficking defects and drugs. *Pharmacol. Ther.* **2013**, *139*, 24–31. [CrossRef]
36. Jansen, J.A.; De Boer, T.P.; Wolswinkel, R.; Van Veen, T.A.; Vos, M.A.; Van Rijen, H.V.; Van der Heyden, M.A.G. Lysosome mediated Kir2.1 breakdown directly influences inward rectifier current density. *Biochem. Biophys. Res. Commun.* **2008**, *367*, 687–692. [CrossRef]
37. Nalos, L.; De Boer, T.P.; Houtman, M.J.; Rook, M.B.; Vos, M.A.; Van der Heyden, M.A.G. Inhibition of lysosomal degradation rescues pentamidine-mediated decreases of $K_{IR}2.1$ ion channel expression but not that of $K_v11.1$. *Eur. J. Pharmacol.* **2011**, *652*, 96–103. [CrossRef]
38. Ohkuma, S.; Poole, B. Fluorescence probe measurement of the intralysosomal pH in living cells and the perturbation of pH by various agents. *Proc. Natl. Acad. Sci. USA* **1978**, *75*, 3327–3331. [CrossRef]
39. Zhou, Z.; Gong, Q.; Ye, B.; Fan, Z.; Makielski, J.C.; Robertson, G.A.; January, C.T. Properties of HERG channels stably expressed in HEK 293 cells studied at physiological temperature. *Biophys. J.* **1998**, *74*, 230–241. [CrossRef]
40. Chakrabarti, S.; Wu, X.; Yang, Z.; Wu, L.; Yong, S.L.; Zhang, C.; Hu, K.; Wang, Q.K.; Chen, Q. MOG1 rescues defective trafficking of Na(v)1.5 mutations in Brugada syndrome and sick sinus syndrome. *Circ. Arrhythm. Electrophysiol.* **2013**, *6*, 392–401. [CrossRef]
41. Fader, C.M.; Colombo, M.I. Autophagy and multivesicular bodies: Two closely related partners. *Cell Death Differ.* **2009**, *16*, 70–78. [CrossRef] [PubMed]
42. Henne, W.M.; Buchkovich, N.J.; Emr, S.D. The ESCRT pathway. *Dev. Cell* **2011**, *21*, 77–91. [CrossRef] [PubMed]
43. Dean, L. Propafenone Therapy and CYP2D6 Genotype. In *Medical Genetics Summaries*; Pratt, V.M., Scott, S.A., Pirmohamed, M., Esquivel, B., Kane, M.S., Kattman, B.L., Malheiro, A.J., Eds.; National Center for Biotechnology Information (US): Bethesda, MD, USA, 2012.

44. Cay, S.; Kara, M.; Ozcan, F.; Ozeke, O.; Aksu, T.; Aras, D.; Topaloglu, S. Propafenone use in coronary artery disease patients undergoing atrial fibrillation ablation. *J. Interv. Card Electrophysiol.* **2022**, *65*, 381–389. [CrossRef] [PubMed]
45. Tamargo, J.; Valenzuela, C.; Delpon, E. New insights into the pharmacology of sodium channel blockers. *Eur. Heart J.* **1992**, *13* (Suppl. F), 2–13. [CrossRef]
46. Delpon, E.; Valenzuela, C.; Perez, O.; Casis, O.; Tamargo, J. Propafenone preferentially blocks the rapidly activating component of delayed rectifier K^+ current in guinea pig ventricular myocytes. Voltage-independent and time-dependent block of the slowly activating component. *Circ. Res.* **1995**, *76*, 223–235. [CrossRef]
47. Abi Samra, F. The clinical use of class IC antiarrhythmic drugs. *J. La. State Med. Soc.* **1989**, *141*, 27–31.
48. Femenia, F.; Palazzolo, J.; Arce, M.; Arrieta, M. Proarrhythmia Induced by Propafenone: What is the Mechanism? *Indian Pacing Electrophysiol. J.* **2010**, *10*, 278–280.
49. Chu, Y.Q.; Wang, C.; Li, X.M.; Wang, H. Propafenone-Induced QRS Widening in a Child With Arrhythmogenic Right Ventricular Cardiomyopathy: A Case Report and Literatures Review. *Front. Pediatr.* **2020**, *8*, 481330. [CrossRef]
50. Tomcsanyi, J.; Tomcsanyi, K. Wide QRS alternans caused by propafenone toxicity. *Acta Cardiol.* **2019**, *74*, 82–83. [CrossRef]
51. Puljevic, D.; Smalcelj, A.; Durakovic, Z.; Goldner, V. The influence of atenolol and propafenone on QT interval dispersion in patients 3 months after myocardial infarction. *Int. J. Clin. Pharmacol. Ther.* **1997**, *35*, 381–384.
52. Keramari, S.; Poutoglidis, A.; Poutoglidou, F.; Kaiafa, G.; Keramaris, M. Propafenone Poisoning of a Female Adolescent After a Suicide Attempt. *Cureus* **2021**, *13*, e16576. [CrossRef]
53. Latini, R.; Barbieri, E.; Castello, C.; Marchi, S.; Sica, A.; Gerosa, G.; Rossi, R.; Zardini, P. Propafenone and 5-hydroxypropafenone concentrations in the right atrium of patients undergoing heart surgery. *Am. Heart J.* **1989**, *117*, 497–498. [CrossRef]
54. Steurer, G.; Weber, H.; Schmidinger, H.; Plass, H.; Frey, B.; Purerfellner, H.; Probst, P. Plasma propafenone concentration in the evaluation of anti-arrhythmic efficacy. *Eur. Heart J.* **1991**, *12*, 526–532. [CrossRef] [PubMed]
55. Manu, P.; Rogozea, L.M.; Dan, G.A. Pharmacological Management of Atrial Fibrillation: A Century of Expert Opinions in Cecil Textbook of Medicine. *Am. J. Ther.* **2022**, *29*, e18–e25. [CrossRef]
56. Goversen, B.; de Boer, T.P.; van der Heyden, M.A.G. Commentary: Reciprocal Modulation of IK1-INa Extends Excitability in Cardiac Ventricular Cells. *Front. Physiol.* **2016**, *7*, 647. [CrossRef]
57. Varghese, A. Reciprocal Modulation of IK1-INa Extends Excitability in Cardiac Ventricular Cells. *Front. Physiol.* **2016**, *7*, 542. [CrossRef]
58. Milstein, M.L.; Musa, H.; Balbuena, D.P.; Anumonwo, J.M.; Auerbach, D.S.; Furspan, P.B.; Hou, L.; Hu, B.; Schumacher, S.M.; Vaidyanathan, R.; et al. Dynamic reciprocity of sodium and potassium channel expression in a macromolecular complex controls cardiac excitability and arrhythmia. *Proc. Natl. Acad. Sci. USA* **2012**, *109*, E2134–E2143. [CrossRef] [PubMed]
59. Utrilla, R.G.; Nieto-Marin, P.; Alfayate, S.; Tinaquero, D.; Matamoros, M.; Perez-Hernandez, M.; Sacristan, S.; Ondo, L.; de Andres, R.; Diez-Guerra, F.J.; et al. Kir2.1-Nav1.5 Channel Complexes Are Differently Regulated than Kir2.1 and Nav1.5 Channels Alone. *Front. Physiol.* **2017**, *8*, 903. [CrossRef] [PubMed]
60. Ponce-Balbuena, D.; Guerrero-Serna, G.; Valdivia, C.R.; Caballero, R.; Diez-Guerra, F.J.; Jimenez-Vazquez, E.N.; Ramirez, R.J.; Monteiro da Rocha, A.; Herron, T.J.; Campbell, K.F.; et al. Cardiac Kir2.1 and NaV1.5 Channels Traffic Together to the Sarcolemma to Control Excitability. *Circ. Res.* **2018**, *122*, 1501–1516. [CrossRef] [PubMed]
61. Perez-Hernandez, M.; Matamoros, M.; Alfayate, S.; Nieto-Marin, P.; Utrilla, R.G.; Tinaquero, D.; de Andres, R.; Crespo, T.; Ponce-Balbuena, D.; Willis, B.C.; et al. Brugada syndrome trafficking-defective Nav1.5 channels can trap cardiac Kir2.1/2.2 channels. *JCI Insight* **2018**, *3*, e96291. [CrossRef]
62. Matamoros, M.; Perez-Hernandez, M.; Guerrero-Serna, G.; Amoros, I.; Barana, A.; Nunez, M.; Ponce-Balbuena, D.; Sacristan, S.; Gomez, R.; Tamargo, J.; et al. Nav1.5 N-terminal domain binding to alpha1-syntrophin increases membrane density of human Kir2.1, Kir2.2 and Nav1.5 channels. *Cardiovasc. Res.* **2016**, *110*, 279–290. [CrossRef] [PubMed]
63. Shieh, R.C.; Chang, J.C.; Arreola, J. Interaction of Ba^{2+} with the pores of the cloned inward rectifier K^+ channels Kir2.1 expressed in Xenopus oocytes. *Biophys J.* **1998**, *75*, 2313–2322. [CrossRef]
64. Hsieh, C.P.; Kuo, C.C.; Huang, C.W. Driving force-dependent block by internal Ba^{2+} on the Kir2.1 channel: Mechanistic insight into inward rectification. *Biophys. Chem.* **2015**, *202*, 40–57. [CrossRef] [PubMed]
65. Clarke, O.B.; Caputo, A.T.; Hill, A.P.; Vandenberg, J.I.; Smith, B.J.; Gulbis, J.M. Domain reorientation and rotation of an intracellular assembly regulate conduction in Kir potassium channels. *Cell* **2010**, *141*, 1018–1029. [CrossRef] [PubMed]
66. Van der Heyden, M.A.G.; Jespersen, T. Pharmacological exploration of the resting membrane potential reserve: Impact on atrial fibrillation. *Eur. J. Pharmacol.* **2016**, *771*, 56–64. [CrossRef]
67. Pegan, S.; Arrabit, C.; Zhou, W.; Kwiatkowski, W.; Collins, A.; Slesinger, P.A.; Choe, S. Cytoplasmic domain structures of Kir2.1 and Kir3.1 show sites for modulating gating and rectification. *Nat. Neurosci.* **2005**, *8*, 279–287. [CrossRef]
68. Caballero, R.; Dolz-Gaiton, P.; Gomez, R.; Amoros, I.; Barana, A.; Gonzalez de la Fuente, M.; Osuna, L.; Duarte, J.; Lopez-Izquierdo, A.; Moraleda, I.; et al. Flecainide increases Kir2.1 currents by interacting with cysteine 311, decreasing the polyamine-induced rectification. *Proc. Natl. Acad. Sci. USA* **2010**, *107*, 15631–15636. [CrossRef]
69. Garneau, L.; Klein, H.; Parent, L.; Sauve, R. Contribution of cytosolic cysteine residues to the gating properties of the Kir2.1 inward rectifier. *Biophys. J.* **2003**, *84*, 3717–3729. [CrossRef]
70. Bandyopadhyay, D.; Cyphersmith, A.; Zapata, J.A.; Kim, Y.J.; Payne, C.K. Lysosome transport as a function of lysosome diameter. *PLoS ONE* **2014**, *9*, e86847. [CrossRef]

71. Piper, R.C.; Luzio, J.P. Late endosomes: Sorting and partitioning in multivesicular bodies. *Traffic* **2001**, *2*, 612–621. [CrossRef]
72. Hu, Y.B.; Dammer, E.B.; Ren, R.J.; Wang, G. The endosomal-lysosomal system: From acidification and cargo sorting to neurodegeneration. *Transl. Neurodegener.* **2015**, *4*, 18. [CrossRef]
73. de Boer, T.P.; van Veen, T.A.; Houtman, M.J.; Jansen, J.A.; van Amersfoorth, S.C.; Doevendans, P.A.; Vos, M.A.; van der Heyden, M.A.G. Inhibition of cardiomyocyte automaticity by electrotonic application of inward rectifier current from Kir2.1 expressing cells. *Med. Biol. Eng. Comput.* **2006**, *44*, 537–542. [CrossRef]
74. Li, E.; Loen, V.; Van Ham, W.B.; Kool, W.; Van der Heyden, M.A.G.; Takanari, H. Quantitative analysis of the cytoskeleton's role in inward rectifier K_{IR}2.1 forward and backward trafficking. *Front. Physiol.* **2021**, *12*, 812572. [CrossRef] [PubMed]
75. Qile, M.; Beekman, H.D.M.; Sprenkeler, D.J.; Houtman, M.J.C.; van Ham, W.B.; Stary-Weinzinger, A.; Beyl, S.; Hering, S.; van den Berg, D.J.; de Lange, E.C.M.; et al. LUF7244, an allosteric modulator/activator of Kv 11.1 channels, counteracts dofetilide-induced torsades de pointes arrhythmia in the chronic atrioventricular block dog model. *Br. J. Pharmacol.* **2019**, *176*, 3871–3885. [CrossRef]
76. Rodriguez-Menchaca, A.A.; Navarro-Polanco, R.A.; Ferrer-Villada, T.; Rupp, J.; Sachse, F.B.; Tristani-Firouzi, M.; Sanchez-Chapula, J.A. The molecular basis of chloroquine block of the inward rectifier Kir2.1 channel. *Proc. Natl. Acad. Sci. USA* **2008**, *105*, 1364–1368. [CrossRef] [PubMed]
77. de Boer, T.P.; Nalos, L.; Stary, A.; Kok, B.; Houtman, M.J.; Antoons, G.; van Veen, T.A.; Beekman, J.D.; de Groot, B.L.; Opthof, T.; et al. The anti-protozoal drug pentamidine blocks KIR2.x-mediated inward rectifier current by entering the cytoplasmic pore region of the channel. *Br. J. Pharmacol.* **2010**, *159*, 1532–1541. [CrossRef]
78. Lee, Y.M.; Thompson, G.A.; Ashmole, I.; Leyland, M.; So, I.; Stanfield, P.R. Multiple residues in the p-region and m2 of murine kir 2.1 regulate blockage by external ba. *Korean J. Physiol. Pharmacol.* **2009**, *13*, 61–70. [CrossRef] [PubMed]
79. Fernandes, C.A.H.; Zuniga, D.; Fagnen, C.; Kugler, V.; Scala, R.; Pehau-Arnaudet, G.; Wagner, R.; Perahia, D.; Bendahhou, S.; Venien-Bryan, C. Cryo-electron microscopy unveils unique structural features of the human Kir2.1 channel. *Sci. Adv.* **2022**, *8*, eabq8489. [CrossRef]
80. Houtman, M.J.C.; Chen, X.; Qile, M.; Duran, K.; van Haaften, G.; Stary-Weinzinger, A.; van der Heyden, M.A.G. Glibenclamide and HMR1098 normalize Cantu syndrome-associated gain-of-function currents. *J. Cell Mol. Med.* **2019**, *23*, 4962–4969. [CrossRef]
81. Hund, T.J.; Koval, O.M.; Li, J.; Wright, P.J.; Qian, L.; Snyder, J.S.; Gudmundsson, H.; Kline, C.F.; Davidson, N.P.; Cardona, N.; et al. A beta(IV)-spectrin/CaMKII signaling complex is essential for membrane excitability in mice. *J. Clin. Investig.* **2010**, *120*, 3508–3519. [CrossRef]